Organic Electronics 50 (2017) 48–54

Contents lists available at ScienceDirect

Organic Electronics

journal homepage: www.elsevier.com/locate/orgel

Impact of defects on exciton diffusion in organic light-emitting diodes

Grayson L. Ingram*, Zheng-Hong Lu

Department of Materials Science and Engineering, University of Toronto, Toronto, M5S 3E4, Canada

ARTICLE INFO

Article history:
Received 1 April 2017
Received in revised form
7 July 2017
Accepted 10 July 2017
Available online 11 July 2017

Keywords:
Exciton diffusion
Electroluminescence
Organic light emitting device
Defect
Singlet

ABSTRACT

The impact of defect concentration and current density on the effective singlet exciton diffusion length in 4'-bis(carbazol-9-yl)biphenyl (CBP) is quantified by analyzing the electroluminescent characteristics of several sets of OLEDs. The defect concentration and effective diffusion length are determined through fitting of the defect and CBP emission bands in the electroluminescence spectra under constant current operation using an analytical model derived based on the competition between exciton diffusion and energy transfer to defects. Defect concentrations of $3 \pm 1 \times 10^{18}$ cm^{-3}, $2 \pm 1 \times 10^{18}$ cm^{-3} and $0.3 \pm 0.7 \times 10^{18}$ cm^{-3} are calculated in three sets of OLEDs, in which the effective diffusion length decreases as the defect concentration increases. Modelling the dependence of the effective diffusion length on defect concentration a "defect free" diffusion length of 4.5 ± 0.3 nm is obtained for CBP singlet excitons in these devices operated under low current density. We also show that the driving voltage scales linearly with the defect concentration.

1. Introduction

The diffusion of bound electron-hole pairs, or excitons, plays an important role in organic optoelectronic devices such as organic photovoltaics and organic light-emitting diodes (OLEDs). In the former, the diffusion of excitons to a dissociating interface is a necessary step in the generation of free charges from absorbed light. In the latter exciton transport determines both efficiency and operational stability of devices. In both applications, the diffusion of excitons in an organic thin film depends strongly on the photophysical properties of the individual molecules, which can be controlled to some extent through molecular design [1–3], as well as the properties of the solid film they form. Systematic studies of how the properties of organic films influence exciton diffusion have analyzed the importance of purity [4–6] and film crystallinity [7–13].

In this work we explore the relationship between the defect concentration and singlet exciton diffusion length in 4'-bis(carbazol-9-yl)biphenyl (CBP). CBP defect formation and its effect on OLED performance have been studied as a result of both operational degradation and post fabrication annealing in OLEDs [14–16], but the impact of CBP defects on exciton diffusion has not yet been considered.

Here, we study the dependence of singlet exciton diffusion on defect concentration in CBP by monitoring the emission of a series of OLEDs with thin exciton capturing layers. CBP defects are emissive, allowing us to quantify the defect concentration through analysis of OLED emission spectra. The origin of varying defect concentrations is not known, however Wang et al. have demonstrated that CBP defects can be produced through thermal annealing [14] and we expect that excess heat produced during either the CBP deposition or during the high temperature cathode deposition may lead to defect formation during device fabrication. Modelling the changes in exciton diffusion as a function of the defect concentration allows us to determine the "defect-free" singlet exciton diffusion length in CBP, analogous to the impurity free exciton diffusion length reported by Curtin et al. in a photoluminescence based study of exciton diffusion in N,N'-bis(naphthalen-1-yl)-N,N'-bis(phenyl)-benzidine (α-NPD) [4].

The method of using exciton capturing layers in an OLED to study exciton diffusion has been demonstrated previously to measure exciton diffusion lengths [17–22]. It has the advantage of probing organic materials under the same fabrication and operational conditions as other organic layers used in real devices.

2. Experimental

The OLED device architecture used in this study is shown in Fig. 1. All OLEDs have the same general structure ITO/MoO_3 (1 nm)/CBP (53-d nm)/CBP:rubrene (3 nm, 2 wt%)/CBP (d nm)/TPBi

* Corresponding author.
E-mail address: grayson.ingram@mail.utoronto.ca (G.L. Ingram).

http://dx.doi.org/10.1016/j.orgel.2017.07.017
1566-1199/

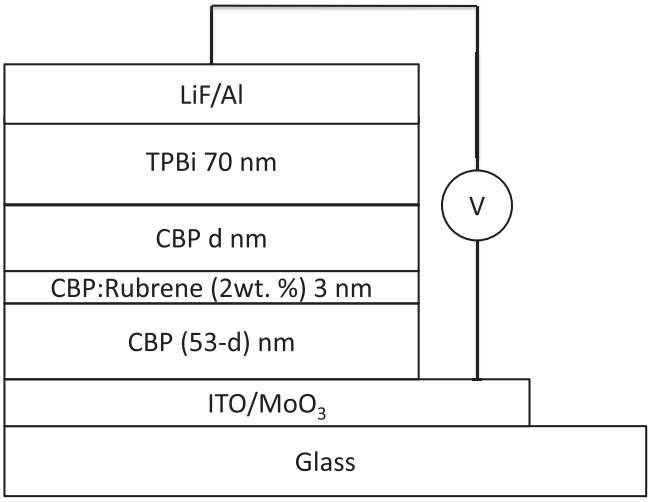

Fig. 1. Schematic device structure of the OLEDs used in this study.

(70 nm)/LiF (1 nm)/Al (100 nm), where CBP is used as the hole transport layer (HTL), and 1,3,5-tris(Nphenylbenzimidazole-2-yl) benzene (TPBi) is used as the electron transport layer (ETL).

Three sets of OLEDs are fabricated, with the distance between the ETL/HTL interface and CBP:Rubrene layer, d, varying across the devices within each set. Each set of OLEDs is fabricated on a single substrate with shared electrodes, injection layers, rubrene doped layer, and electron transport layer, while CBP layers of varying thickness are deposited before and after the CBP:rubrene layer to vary the position of the rubrene doped layer in the device, while keeping the total device thickness constant. Each set of devices is fabricated entirely under vacuum (except for the pre-patterned ITO anode) with varying thickness of the CBP layers enabled using a set of interchangeable shadow masks. Although the three sets of devices investigated are nominally identical, we find evidence of varying defect concentration between the three sets (see Section 4). To ensure that the variation in defect concentration only occurs between the sets of devices and not between the layers of a given set, we fabricate two control devices with the structure: ITO/MoO_3 (1 nm)/CBP (45 nm)/CBP (10 nm)/TPBi (70 nm)/LiF (1 nm)/Al (100 nm). All layers of the two devices are shared except for the 10 nm CBP layer which was deposited individually for each of the two devices. The emission spectrum of the two devices are identical (see supplementary Figure S1), confirming that layer-to-layer variations in defect concentration are not significant within a set of devices fabricated on a single substrate.

Although we cannot verify the mechanisms leading to the defect formation in these nominally identical sets of devices, it may be due to the samples' inadvertent exposure to heat or light during the fabrication process and while being stored prior to testing. Alternatively, if defects arise due to CBP aggregation into a more thermodynamically favorable state as proposed by Wang et al. [14], defect formation may occur over time even in the absence of stressors such as heat or light. We note that the diversity in photoluminescence spectra [23–25] reported for CBP suggests that variations in CBP film composition are common.

The rubrene doped CBP is included to capture singlet excitons which diffuse from the exciton formation region at the ETL/HTL interface. The low singlet energy of the rubrene dopants ensures that any excitons diffusion to the layer are quickly captured, while the higher singlet energy of TPBi relative to CBP confines excitons to the CBP layer. Varying the position of this exciton capturing layer allows for the systematic variation of the singlet exciton concentration.

Samples were fabricated on pre-patterned ITO coated glass in a Kurt J. Lesker Luminos Clustertool with a base pressure of ~10^{-8} Torr. Prior to deposition, the substrates were cleaned with a standard regiment of Alconox®, acetone, and methanol, followed by UV ozone treatment for 15 minutes. Layer thicknesses were measured in-situ using a quartz crystal monitor, and calibrated by profilometry using a KLA-Tencor P16+.

Current-voltage data was measured using a Keithley 6430. OLED spectra were collected using an integrating sphere connected by optical fiber to an Ocean Optics USB4000 spectrometer. All measurements are made in ambient conditions.

3. Theory

The singlet exciton population in the CBP layer of the OLED structure described above, under constant current operation can be modelled using the steady state diffusion equation.

$$0 = D\frac{\partial^2 n(x)}{\partial x^2} - \frac{n(x)}{\tau} - k_{ET} n(x) N \tag{1}$$

n(x) is the CBP singlet exciton concentration, x is the position in the device measured from the ETL/HTL interface towards the anode, D is the CBP singlet diffusivity, τ is the singlet exciton natural lifetime, k_{ET} is the average energy transfer rate of singlets from the CBP to the defects, and N is the defect concentration, which is assumed to be uniform. The terms in Equation (1) from left to right correspond to exciton diffusion, exciton decay and energy transfer to defects.

We express Equation (1) in a simpler form in Equation (2).

$$0 = \frac{\partial^2 n(x)}{\partial x^2} - \frac{n(x)}{L_{eff}^2} \tag{2}$$

The true diffusion length, $L = \sqrt{D\tau}$, is defined as the diffusion length in the absence of any defects and is related to the effective diffusion length, L_{eff}, through Equation (3).

$$L_{eff} = \frac{L}{\sqrt{1 + \tau k_{ET} N}} \tag{3}$$

If the defect concentration increases, the effective diffusion length will decrease due to increased competition between singlet exciton diffusion and energy transfer to defects.

Equation (2) can be solved using the boundary conditions in Equations (4) and (5). Equation (4) represents singlet exciton formation localized at the CBP/TPBi interface by equating the exciton flux at this interface to the rate of charge injection:

$$-D\left.\frac{\partial n}{\partial x}\right|_0 = \frac{J}{4e} \tag{4}$$

J is the current density and e is the elementary charge. The factor of ¼ on the right side of Equation (4) is equal to the fraction of excitons which are produced in the singlet state under electrical excitation. A previous study shows a narrow exciton generation zone for this device structure [26] which is why we localize exciton formation to the ETL/HTL interface here.

Equation (5) represents complete energy transfer of singlet excitons to the rubrene at the boundary of the exciton capturing layer positioned at a distance d from the ETL/HTL interface, as discussed in the Supplementary Information of Ref. 23:

$$n(d) = 0 \tag{5}$$

d is the position of the exciton capturing layer as measured from